

Induction of t(11;14) IgH enhancer/promoter-*cyclin D1* gene translocation using CRISPR/Cas9

NAOHIRO TSUYAMA¹, YU ABE¹, AKI YANAGI¹, YUKARI YANAI¹, MISAKI SUGAI¹,
ATSUSHI KATAFUCHI¹, FUMIHIKO KAWAMURA¹, KENJI KAMIYA² and AKIRA SAKAI¹

¹Department of Radiation Life Sciences, Fukushima Medical University, Fukushima 960-1295;

²Department of Experimental Oncology, Research Institute for Radiation Biology and Medicine,
Hiroshima University, Minami-ku, Hiroshima 734-8553, Japan

Received September 7, 2018; Accepted April 18, 2019

DOI: 10.3892/ol.2019.10303

Abstract. Chromosomal translocation is a key process in the oncogenic transformation of somatic cells. Previously, artificial induction of chromosomal translocation was performed using homologous recombination-mediated loxP labeling of target regions followed by Cre-mediated recombination. Recent progress in genome editing techniques has facilitated the easier induction of artificial translocation by cutting two targeted genome sequences from different chromosomes. The present study established a system to induce t(11;14)(q13;q32), which is observed primarily in multiple myeloma (MM) and involves the repositioning of the *cyclin D1* (*CCND1*) gene downstream of the immunoglobulin heavy chain (IgH) constant region enhancers by translocation. The placing of tandem gRNAs designed to cut both the *IgH E μ* and *CCND1* 15-kb upstream regions in lenti-CRISPRv2 enabled the induction of chromosomal translocation in 293T cells, with confirmation by translocation-specific PCR and fluorescence *in situ* hybridization probing with *IgH* and *CCND1*. At the translocation junctions, small deletions and the addition of DNA sequences (indels) were observed in several clones. Cloned cells with t(11;14) exhibited slower growth and lower *CCND1* mRNA expression compared to the parent cells, presenting the opposite phenomena induced by t(11;14) in MM cells, indicating that the silent *IgH* gene juxtaposed to *CCND1* may negatively affect *CCND1* gene expression and cell proliferation in the non-B lymphocyte lineage. Therefore, the present study achieved the induction of silent promoter/enhancer translocation in t(11;14)(q13;q32) as a preparatory experiment to study the role of *IgH* constant region enhancer-driven *CCND1* overexpression in oncogenic transformation processes in B lymphocytes.

Introduction

Chromosomal translocations have been detected in a variety of cancers. Certain types of translocation are known to cause specific cancers. Translocations include several types of fusion genes, for example, fusion genes in which a chimeric open reading frame produces a chimeric protein after inter-intronic recombination between two different genes, and promoter/enhancer translocation upstream of a different gene, with subsequent control of expression by the translocated promoter/enhancer (1,2).

Among fusion genes involved in hematopoietic malignancies, the first to be cloned was the *BCR/ABL* fusion gene from the Philadelphia chromosome, t(9;22), associated with chronic myelogenous leukemia, although dozens of translocated genes were already identified (3). Multiple myeloma (MM) results from malignantly transformed plasma cells and is reportedly associated with specific translocations, such as t(11;14), t(4;14), and t(14;16) (4–6). As a common feature, the enhancer region of the immunoglobulin heavy chain (*IgH*) gene is rearranged to the target gene; transcriptional activation of the gene in a B lymphocyte-specific manner results in its functioning as an oncogene. The most frequently detected translocation in MM is rearrangement between the constant region of the *IgH* gene on the long arm of chromosome 14 and the 5'-upstream region of the *cyclin D1* (*CCND1*) gene on the long arm of chromosome 11. Similar translocations were initially identified in the locus of *B-cell CLL/lymphoma 1* (*Bcl1*) in t(11;14)(q13;q32) (7,8). *CCND1* is a key molecule of the cell cycle control machinery, involved in regulating the G1/S transition process (9). Cyclin activity is controlled by transcription level. In the middle of the G1 phase, transcriptional activation of the *cyclin D1* gene results in an increase in protein production, which then complexes with and induces the kinase activity of cdk4 and cdk6, in turn stimulating cell cycle progression. *CCND1* gene juxtaposed to the downstream of *IgH* constant region shows accelerated expression of *CCND1* proteins by the effect of *IgH* super-enhancer in B lymphocyte-specific manner, therefore, t(11;14)-harboring cells indicate increased cell proliferation (10).

Sequencing of the junction point of t(11; 14)(q13; q32) in B-cell malignancies revealed a difference between

Correspondence to: Dr Naohiro Tsuyama, Department of Radiation Life Sciences, Fukushima Medical University, Hikarigaoka 1, Fukushima 960-1295, Japan
E-mail: tsuyama@fmu.ac.jp

Key words: multiple myeloma, CRISPR/CRISPR-associated protein 9, t(11;14)(q13;q32), immunoglobulin H enhancer, *cyclin D1*

B-cell lymphoma and MM (4,11,12). Two types of gene rearrangement mechanisms are involved in chromosomal translocations associated with B-cell malignancies: one that involves VDJ recombination mediated by *recombination activating gene (RAG)1/2*, and another that involves *activation-induced cytidine deaminase (AID)* in immunoglobulin class switching processes (3). Translocation in MM is induced by *AID* (13,14). The resulting differences in the origin of translocation-containing malignant cells in various B-cell differentiation stages cause differences in clinical condition (4,15).

Genome editing systems are now widely utilized in many research fields (16,17). Among these systems, the *Streptococcus pyogenes* type II clustered, regularly interspaced, short palindromic repeats (CRISPR)-Cas9 system enables efficient sequence-specific editing, enhancing the homologous recombination-mediated template replacement of target genes (18-20). Software that provides for effective visual target estimation of CRISPR/Cas9 in the genome database in combination with an evaluation score enhances the convenience of the system (21). Recent reports have described the induction of chromosomal translocations by simultaneous cutting of two specific DNA sequences using CRISPR-Cas9 (22-27) to engineer translocations that produce chimeric proteins from the fusion genes. Translocation of promoter/enhancer regions such as the B-cell lymphoma t(11;14) has not been reported, however.

In this study, we developed a CRISPR/Cas9-mediated genome editing system to induce the MM-specific chromosomal translocation t(11;14)(q13;q32) in cultured cells and confirmed the induction of a translocation identical to the experimental design. In addition, we analyzed the DNA sequence of the translocation junction, the gene expression and growth characteristics of t(11;14)-positive cells.

Materials and methods

Materials. Cell culture reagents, Dulbecco's modified Eagle's medium (DMEM) and penicillin/streptomycin, were obtained from Nakalai Tesque (Kyoto, Japan). Plasmids used in this study, lentiCRISPRv2 (#98290), pCAG-EGxxFP (#50716) (28), pX330 Cctn1/1 (#50718), and pCAG-EGxxFP-Cctn1 (#50717), were obtained from Addgene (www.addgene.org). lentiCRISPRv2 puro was a gift from Brett Stringer. Synthetic oligonucleotides were obtained from Eurofin Genomics (Tokyo, Japan). DNA iso, RNAiso, Guide-it mutation detection kit, and pMD20-T TA cloning vector were purchased from Takara bio (Kyoto, Japan). Thunderbird® SYBR qPCR Mix, KOD-PLUS, and ReverTraAce were obtained from Toyobo (Tokyo, Japan). PEImax 40000 was obtained from Polyscience Inc. (Warrington, PA, USA).

Cell culture, transfection, and virus packaging. 293 and 293T (SV40 T antigen introduced 293, 293T) cells originated from Japanese Collection of Research Bioresources Cell Bank were cultured in Dulbecco's modified Eagle medium containing 10% fetal calf serum and incubated in a humidified chamber at 37°C with 95% air and 5% CO₂. These cells were confirmed to be mycoplasma free. Plasmid transfection was carried out using PEImax 40000, following the

manufacturer's protocol. For lentivirus packaging, plasmids were introduced into 293T cells, with subsequent recovery of the culture supernatant. Virus particles were recovered by centrifugation of the supernatant following addition of PEG6000 and NaCl (29).

CRISPR target localization. CRISPRscan (www.crisprscan.org/) (21) was used to localize the 20-bp target sequences of the *IgH Eμ* region and *CCND1* gene 5'-upstream region on the UCSC genome browser (<http://www.ucsc.genome.edu/>). Candidate gRNAs without potential off-targets were selected using Cutting Frequency Determination score (30) indicated by CRISPRscan.

Plasmid construction. Double-stranded oligonucleotides for the guide RNA of *IgH Eμ* (5'-CACCGGACTGGCCTAGCG GAGGCTC-3' and 5'-AAACGAGCCTCCGCTAGGCCA GTCC-3' for candidate A, 5'-CACCGGAGAACATACCAA GCCCAC-3' and 5'-AAACGTGGGGCTTGGTATGTT CTCC-3' for candidate B) and *CCND1* (5'-CACCGGGGG TAGGAAGCCTCGGCTGTGG-3' and 5'-AAACCCACAGCC GAGGCTTCCTACCCCC-3' for candidate A, 5'-CACCGG TGGCGAGGTGGGACCGCGG-3' and 5'-AAACCCGCG GTCCCACCTCGCCACC-3' for candidate B) were ligated into lentiCRISPRv2 vector digested with *BsmBI*. For construction of pCAG-EGxxFP vectors to monitor gRNA activity, *IgH* or *CCND1* gene target sequences were PCR-amplified from 293T cell genomic DNA using 5'-TTAGACAAGGGCGAT GCCAG-3' and 5'-TCAAGACCACTTTTCAACTACTCAC-3' for *IgH* candidate A, 5'-TCATTACCACCTCCACTACCT-3' and 5'-CCACTAGAAGGGGAAGTGGTC-3' for *IgH* candidate B, 5'-CACATGCCCCGAAGTCAAACC-3' and 5'-ATC ACCGAGATCAGAAGGCT-3' for *CCND1* candidate A, and 5'-CTTCTCACGAGCTGCCTTTG-3' and 5'-GCTCATCAC ACAGCTTGACG-3' for *CCND1* candidate B with KOD-Plus DNA polymerase. After cloning into pMD20-T for DNA sequence confirmation, the target sequences were cloned into the pCAG-EGxxFP cleavage site. For the *IgH-CCND1* tandem-lentiCRISPRv2 vector, the U6-*IgH* gRNA B expression cassette cloned into pMD20-T was PCR-amplified from *IgH-B* lentiCRISPRv2 using 5'-GCAGAGATCCAGTTTGGT TAAT-3' and 5'-ACCTAGCTAGCGtATTCAAAAA-3' with KOD-Plus DNA polymerase and then cloned into *CCND1* B lentiCRISPRv2.

Homology-directed repair (HDR)-mediated EGxxFP repair monitoring of gRNA activity. *IgH* or *CCND1* gRNA activity was monitored according to a previous report (28). Briefly, *IgH* (or *CCND1*, *IgH-CCND1* tandem) lentiCRISPRv2 and pCAG-EGxxFP *IgH* (or *CCND1*) vectors were co-transfected into 293T cells. Two days later, EGFP fluorescence was observed using a fluorescence microscope (Axio Vert.A1, Zeiss, Oberkochen, Germany) and a flow cytometer (S3e cell sorter, Bio-Rad, Hercules, CA, USA). The fluorescence of co-transfected cells was compared to that of the positive control, pX330-Cctn1/1 and pCAG-EGxxFP Cctn1 combination, and the negative control, empty lentiCRISPRv2 and pCAG-EGxxFP. In flow cytometric analyses, mean fluorescence intensity of GFP-positive live cells was obtained using forward/side scatter-gating and FL1 window.

Confirmation of CRISPR genome editing activity. The genome editing activity of the *IgH-CCND1* CRISPR vectors was confirmed by infecting 293T and 293 cells with lenti-CRISPRv2 virus. These cells were selected as previous reports successfully established artificial translocation using CRISPR/Cas9 (22,25). Cells were infected with virus suspension and cultured for 14 days with puromycin. Colonies were picked, and DNA was recovered using a DNAiso kit according to the manufacturer's protocol. The genome regions of gRNA target sites were then PCR-amplified from puromycin-selected cells and parent cells using the primers used in EGxxFP vector construction. A Guide-IT mutation detection kit was used to detect mutations introduced into the genomic DNA of CRISPR target sites. Purified PCR products of selected and parental origin were mixed equivalently, denatured, reannealed, incubated with Guide-it nuclease, and electrophoresed to detect mismatch-directed cleavage. In addition, to confirm genome editing at DNA sequence level, PCR-amplified fragments were recombined into the pMD20-T TA cloning vector, and inserted DNA was sequenced by Fasmac Co. (Kanagawa, Japan).

Confirmation of translocation. PCR confirmation of translocation was performed using the *IgH/CCND1* translocation specific primer pair (5'-AAGGGTGCATGATGACCTAC-3' for *IgH* side and 5'-AGCTGTTCTTGTAGTGCC-3' for *CCND1* side) with Thunderbird® SYBR qPCR Mix and a Light Cycler Nano (Roche Diagnostics, Basel, Switzerland). For calibration of DNA content in quantitative PCR (Q-PCR), primers for ACTB gene (5'-AGAAAATCTGGCACCACA CC-3' and 5'-AACGGCAGA AGAGAGAACCA-3') were used for reference. PCR condition was, denaturation of template: 94°C 120 sec, DNA amplification cycles: 50 cycles of (94°C 10 sec-62°C 10 sec-72°C 20 sec), melting temperature measurement: 72°C to 94°C at 0.1°C/sec. The presence of translocation-positive clones was assessed based on the melting temperature of PCR-amplified DNA compared with the positive control DNA. To confirm the efficiency of *IgH/CCND1* CRISPR/Cas9-induced translocation, translocation-specific Q-PCR was performed using DNA of *IgH/CCND1* lenti-CRISPRv2-infected cells. Positive control DNA was amplified from genomic DNA 5'-TCATTACCACCCTCCACTAC-3' and 5'-TTTGCTAGCCACTGGCATCGCCCT-3' for the *IgH* side and 5'-GCTCATCACACAGCTTGACG-3' and 5'-TTT GCTAGCGCGGTGGGGTCTTGTGTG-3' for the *CCND1* side, and the two PCR-amplified fragments were recombined into a translocation-mimic PCR template (5'-*IgH-CCND1*-3'). PCR-amplified DNA of candidate positive cells was cloned into TA cloning vector, and inserted DNA was sequenced. DNA sequence alignment was performed using Ape (<http://jorgensen.biology.utah.edu/wayned/ape/>).

RT-qPCR. RNA was isolated from sub-confluent cultures of 293T and t(11;14) positive cells two days after inoculation using RNAiso reagent according to the manufacturer's instructions. cDNAs were synthesized from total RNA using random primers and RevTraAce reverse transcriptase. Quantitative PCR (Q-PCR) was performed using the primers 5'-GAC CCCGACGATTTTCATTG-3' and 5'-CTCTGGAGAGGA AGCGTGTG-3' for *CCND1* and 5'-ACACTTCTGCTCGTT GCCTT-3' and 5'-ACACAAATGCTCCTCTCACC-3' for

MYEOV as the target and 5'-CACCAGGGCTGCTTTTAA CTCT-3' and 5'-TGGGATTTCCATTGATGACAAG-3' for *GAPDH* as the reference with Thunderbird qPCR mix and a LightCycler Nano (n=3) using the same condition to DNA Q-PCR described above. Ratio of 2^{-ΔΔCq} values were calculated from the values obtained by LightCyclerNano Software (31).

Growth curve analysis. A total of 5x10⁴ cells were inoculated into 35-mm dishes and cultured. The number of viable attached cells was determined using a dye-exclusion assay with trypan blue (n=3).

Statistical analysis. Quantitative data were presented as mean ± standard deviation obtained from three independent replicates. Statistical analyses were performed using Welch's t-test on Microsoft Excel version 14 on Windows 7. P<0.05 was considered to indicate a statistically significant difference.

Results

Construction of *IgH/cyclinD1*-specific CRISPR/Cas9. According to the scheme to obtain artificial induction of t(11;14) by cutting *CCND1* upstream on chromosome (chr) 11 and *IgH Eμ* and *Iμ* regions on chr 14 (Fig. 1A), we designed two efficient gRNA sequences to express in one CRISPR/Cas9 vector (Fig. 1B) as described below. In order to mimic t(11;14) in MM (Fig. 1C), we searched target sequences of CRISPR/Cas9 around the previously reported junction sequence (32) using CRISPR Scan. As Ronchetti *et al* (32) were unable to identify clear clustering of junction sites of *CCND1*, we searched the targets from 10 to 20 kb upstream of the protein-coding sequence. For *IgH* genes, *Eμ* and *Iμ* regions were searched. Candidate gRNA sequences predicted to exhibit high editing activity with minimal off-target activity were obtained. Four gRNA target sequences were selected for *IgH* and *CCND1* genes, and synthetic oligonucleotides of these gRNA candidates were recombined into lentiCRISPRv2.

The potency of gRNA sequences was monitored using pCAG-EGxxFP. Both gRNA-coding lentiCRISPRv2 (*IgH*-A, -B, *CCND1*-A or -B) and corresponding gRNA target sequence-containing pCAG-EGxxFP (*IgH*-A, -B, *CCND1*-A or -B) were introduced into 293T cells, and editing activity was observed by recovery of EGFP fluorescence after HDR (Fig. 2A). EGFP fluorescence of cells into which the candidates were introduced was compared to that of positive control cells into which mouse *Cetn1/1* pX330 and pCAG-EGxxFP *Cetn1* were introduced, and candidates exhibiting fluorescence similar to that of *Cetn1/1* cells were chosen (Fig. 2B). By comparing two gRNA candidates A and B for *IgH* or *CCND1*, selected gRNA sequences were 5'-GAGAACATACCAAGC CCCACTGG-3' (*IgH*-B) for *IgH*, Chr14 genome position 105861042-105861064 in Genome Reference Consortium Human 38 (GRCh38), and 5'-GTGGCGAGGTGGGACCGC GGTGG-3' (*CCND1*-B) for *CCND1*, Chr11 genome position 69627757-69627779 in GRCh38 (underlined sequences indicate protospacer adjacent motif, PAM).

To induce chromosomal translocation with a single vector capable of editing both *IgH* and *CCND1*, the U6-*CCND1* gRNA portion of *CCND1*-B lentiCRISPRv2 was PCR-amplified and cloned downstream of the U6-*IgH* gRNA of *IgH*-B

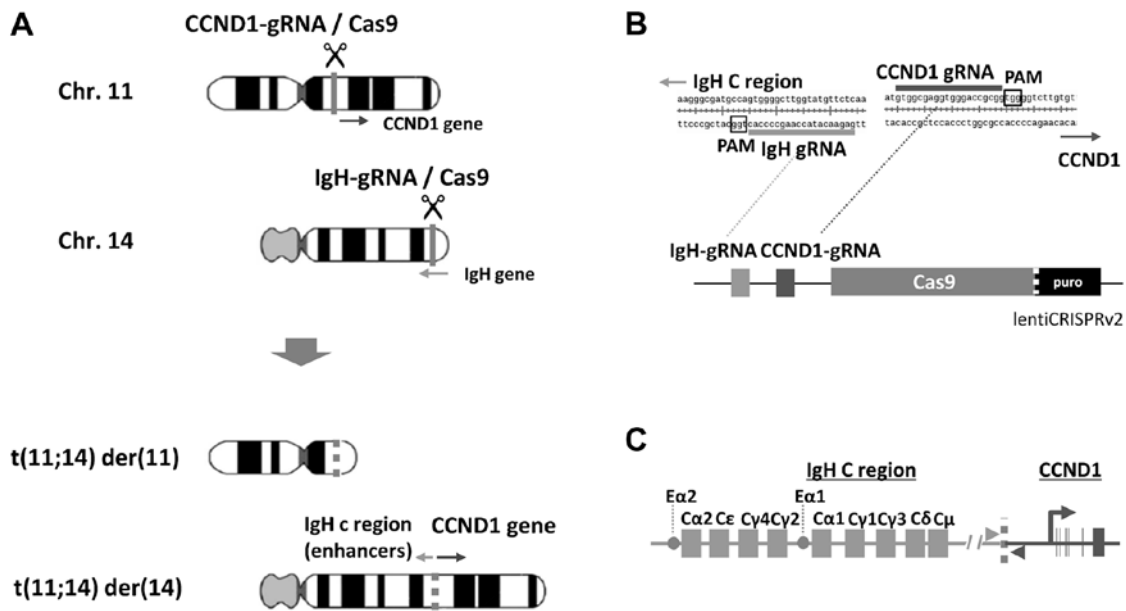


Figure 1. Experimental design of t(11;14). (A) Schematic illustration of *IgH-CCND1* CRISPR/Cas9-mediated induction of t(11;14). (B) gRNA target sequences and tandem-gRNA vector design. (C) Schematic illustration of the *IgH-CCND1* fusion gene. *CCND1* expression is driven by *IgH* C region enhancers in B lymphocytes. Two gray arrowheads at the junction (thick gray dotted line) indicate primer positions used for detection of fusion gene. IgH, immunoglobulin heavy chain; *CCND1*, cyclin D1; Chr, chromosome.

lentiCRISPRv2 (Fig. 1B). The tandem gRNA (*IgH-CCND1*) lentiCRISPRv2 vector exhibited activity similar to that of EGxxFP fluorescence recovery compared with the *IgH* or *CCND1* single-target vectors using *IgH*-B or *CCND1*-B EGxxFP vectors (Fig. 2C). There were some differences of activities between single and tandem gRNA vectors because of unknown reasons. However, we could detect similar activities to that of the positive control reproducibly using these vectors.

Induction of chromosomal translocation. The dual gRNA lentiCRISPRv2 vector was packaged into a lentivirus to observe its translocation inducing activity, and then 293T cells were infected with the virus. Puromycin resistant cells were isolated after seven days. Genome editing activity was confirmed using a mismatch cleavage assay with PCR-amplified *IgH* and *CCND1* genome regions from the DNA of puromycin-resistant cells. Mismatch cleavages by Guide-IT nuclease were indicated in vector-containing cells, demonstrating that Cas9-mediated double-strand breaks and repair by non-homologous end joining (NHEJ) had occurred (Fig. 3A). Translocation-specific PCR was then performed to confirm the presence of the designed translocation in puromycin-resistant cell DNA. Q-PCR analysis using translocation control DNA as the reference revealed a ratio of translocation-positive cells of 1/2,400 in 293T cells, whereas the ratio was 1/70 in 293 cells. Then, DNA bands of the expected length in translocation-positive cells were isolated and cloned into the TA vector, and the DNA sequence of several clones was determined. The observation of characteristic insertion and deletion of several base pairs in the DNA sequencing results for six clones showed that NHEJ had occurred (Fig. 3B). In addition, *IgH* and *CCND1* gRNA target regions in the non-translocated allele were also PCR-amplified and cloned. DNA sequence of four clones

each for *IgH* and *CCND1* had small deletions showing that genome editing occurred even in the non-translocated alleles (data not shown).

To clone translocation-positive 293T cells, Q-PCR was first used to identify wells containing positive cells in 48-well plates inoculated with 200 cells/well. Positive wells were then reseeded at 20 cells/well in 24-well plates, with subsequent identification of wells containing positive cells by Q-PCR as described above. Positive wells were inoculated into dishes at 100 cells/dish, and single colonies were then picked and expanded. We ultimately succeeded in isolating translocation-positive 293T cells using this serial dilution and PCR confirmation approach (data not shown). Direct sequencing of translocation-specific PCR products showed that the junction points of t(11;14) der(11) with the Chr11 centromere and der(14) with the Chr14 centromere were 3 bp from the PAM sequences shown in Fig. 3A. As reported, the Cas9 editing site is 3 bp from the PAM; direct rejoining occurred after editing in this cell clone. Reciprocal chromosomal translocation was also confirmed by fluorescence in situ hybridization (FISH) probing (*IgH* [green] and *CCND1* [red] in Fig. 4B). In triploid karyotype of 293T cells, only one pair of chromosome 11 and 14 was engaged with t(11;14), whereas other two were not.

Characteristics of t(11;14)-positive cells. *IgH* enhancer-driven *CCND1* overexpression by t(11;14) is one of the key factors in oncogenic cell proliferation in MM cells, because the immunoglobulin genes are highly active to produce antibodies only in the B lymphocyte lineage. Therefore, it is difficult to observe *IgH* enhancer-mediated activation of *CCND1* gene unless the cells with t(11;14) differentiate to B lymphocytes. However, silent *IgH* gene in other cell species including 293, which is embryonal kidney origin, may negatively affect

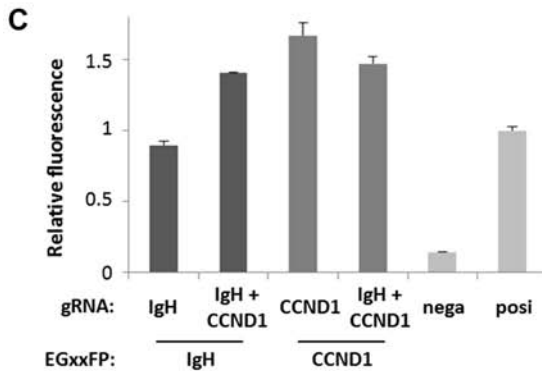
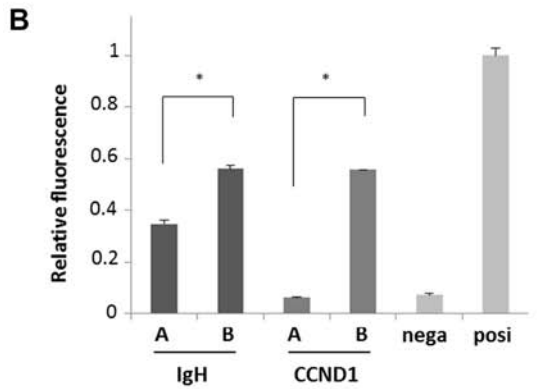
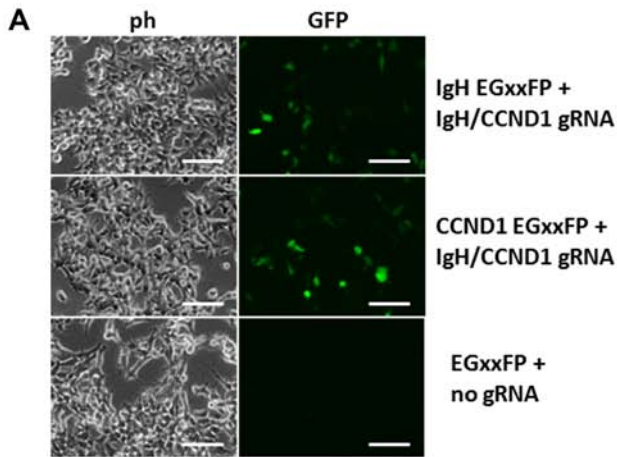


Figure 2. Confirmation of DNA cutting activity of the gRNA candidates. (A) 293T cells were introduced with target DNA (*IgH*, *CCND1* or empty)-containing EGxxFP and gRNA (*IgH* and *CCND1* or empty) expressing lentiCRISPRv2 vectors. Cells with high fluorescence indicate efficient gRNA activity to cut target DNA region. Scale bars, 50 μ m. (B) gRNA activity are compared among *IgH* and *CCND1* gRNA candidates-coding lentiCRISPRv2. Bars A and B indicate the negative control (empty lentiCRISPRv2) and positive control (pX330 *Cetn1*), respectively. Every gRNA vector was co-transfected with the gRNA target DNA-containing EGxxFP vector, and the intensity of cell fluorescence was analyzed by flow cytometry. Relative fluorescence compared to positive control is indicated (n=3). *IgH*-B and *CCND1*-B exhibited stronger fluorescence compared to *IgH*-A and *CCND1*-A, respectively. *P<0.001, as indicated. (C) Activity of single (*IgH*-B or *CCND1*-B) gRNA and dual (*IgH*-B and *CCND1*-B) gRNA expressing vectors were compared by co-transfecting with the gRNA target DNA-containing EGxxFP vectors (indicates as EGxxFP:). Negative and positive controls are the same as those in 2B. IgH, immunoglobulin heavy chain; CCND1, cyclin D1; ph, phase contrast micrograph; GFP, green fluorescent protein; nega, negative; posi, positive.

neighboring gene expression (33). And it is possible that such macroscopic changes induced by chromosomal translocation could alter the cellular characteristics through gene

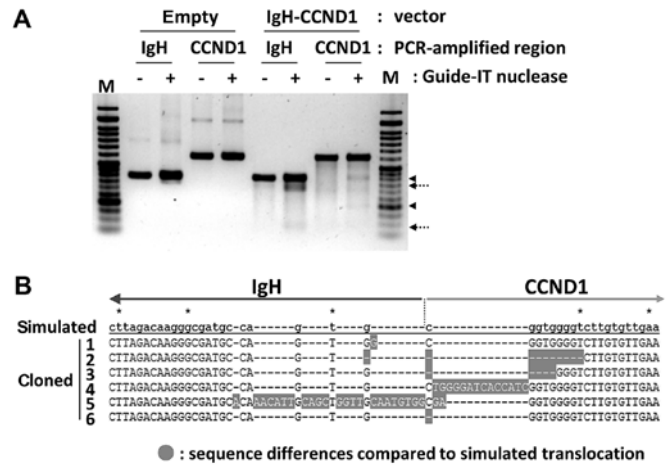


Figure 3. Confirmation of genome editing activity in *IgH* and *CCND1* loci and induced translocation. (A) *IgH* and *CCND1* target regions were PCR-amplified from infected 293T cells and forced using a mismatch cleavage assay. Fragments cleaved by Guide-IT nuclease are indicated by arrows with dotted lines (*IgH*), and arrowheads (*CCND1*). (B) t(11;14) translocation-specific PCR products from infected cells were cloned into the TA cloning vector, followed by DNA sequencing. Sequences of 6 clones are aligned against the simulated *IgH/CCND1* sequence. The junction between *IgH* and *CCND1* is indicated by a dotted line. Sequence differences relative to the simulated sequence are highlighted in gray boxes. IgH, immunoglobulin heavy chain; CCND1, cyclin D1; empty, empty lentiCRISPRv2-introduced; IgH-CCND1, IgH-CCND1 lentiCRISPRv2-introduced; IgH and CCND1 groups, PCR-amplified regions; - and +, Guide-IT nuclease addition; M, DNA marker.

expression. Accordingly, we compared the cell proliferation rate and *CCND1* gene expression in t(11;14)-positive cells to that of parental 293T cells. As shown in Fig. 5A, t(11;14)-positive cells exhibited slower proliferation than 293T cells. A comparison of gene expression of the *CCND1* using *GAPDH* as control by RT-Q-PCR revealed lower *CCND1* expression in the t(11;14)-positive cells compared with parental 293T cells (Fig. 5B). As a previous report suggested that the level of *CCND1* expression is positively correlated with cell proliferation (34), it is possible that decreased *CCND1* expression caused by the silent *IgH* enhancer repositioned in the upstream of *CCND1* gene in t(11;14)-positive cells could result in slower growth compared with parental 293T cells in strong contrast to MM cells. In addition, *MYEOV* gene which locates in the upstream of *CCND1* gene and is often overexpressed in MM cells by the translocated *IgH* variable region in t(11;14) der(11) (35) was also analyzed. But we couldn't detect *MYEOV* gene expression by RT-PCR both in t(11;14)-positive cells and parental 293T cells because of the restricted expression of this gene (gtportal.org/home/gene/ENSG00000172927.3, The Genotype-Tissue Expression database).

Discussion

In this study, we successfully induced artificial chromosomal translocation between the *IgH* constant region promoter/enhancer and the *CCND1* protein-coding region using an *IgH* and *CCND1*-specific CRISPR/Cas9 genome editing system. In contrast to previous reports describing induction of growth-enhancing fusion genes using

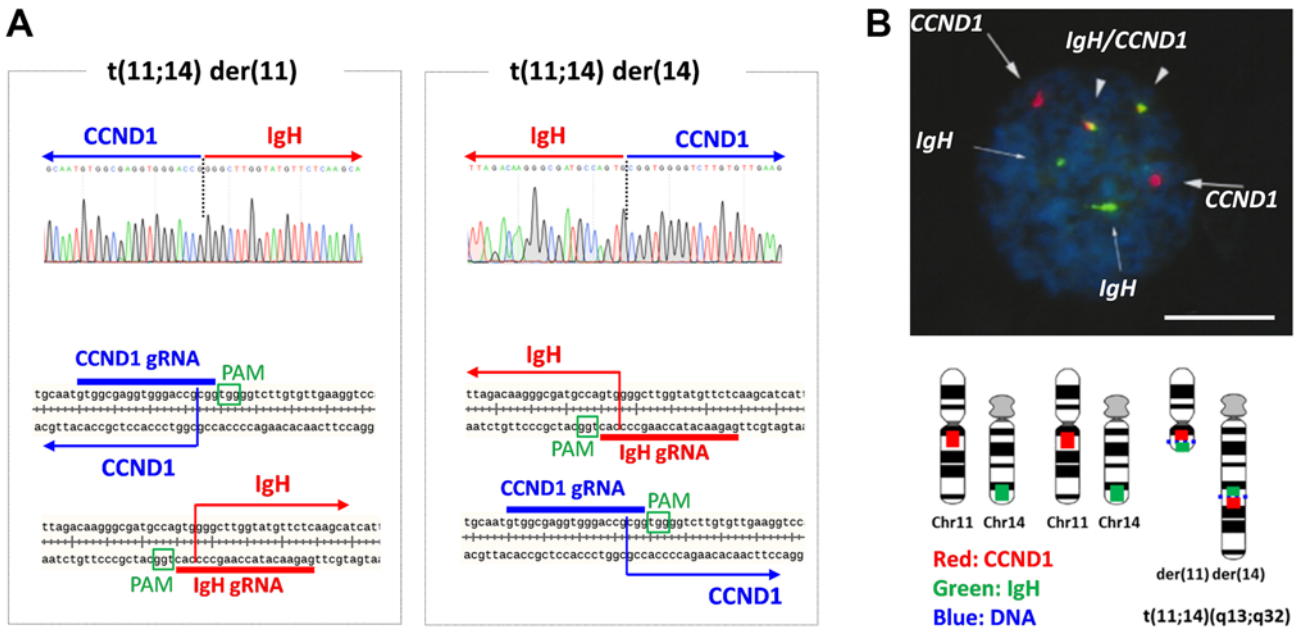


Figure 4. Characterization of *IgH-CCND1* CRISPR/Cas9-induced t(11;14). (A) t(11;14) translocation-specific PCR products from cloned cells were directly sequenced. Junctions in the sequence diagrams are indicated by dotted lines. *CCND1* and *IgH* genome sequences included in der(11) and der(14) are indicated by blue (*CCND1*) and red (*IgH*) arrows with gRNA sequences. (B) t(11;14)-specific fluorescence *in situ* hybridization. One of the triploid Chr11 and Chr14 was reciprocally translocated. *CCND1* and *IgH* probes are labeled with red and green boxes, respectively. Scale bar, 5 μ m. PAM, protospacer adjacent motif; IgH, immunoglobulin heavy chain; CCND1, cyclin D1; Chr, chromosome.

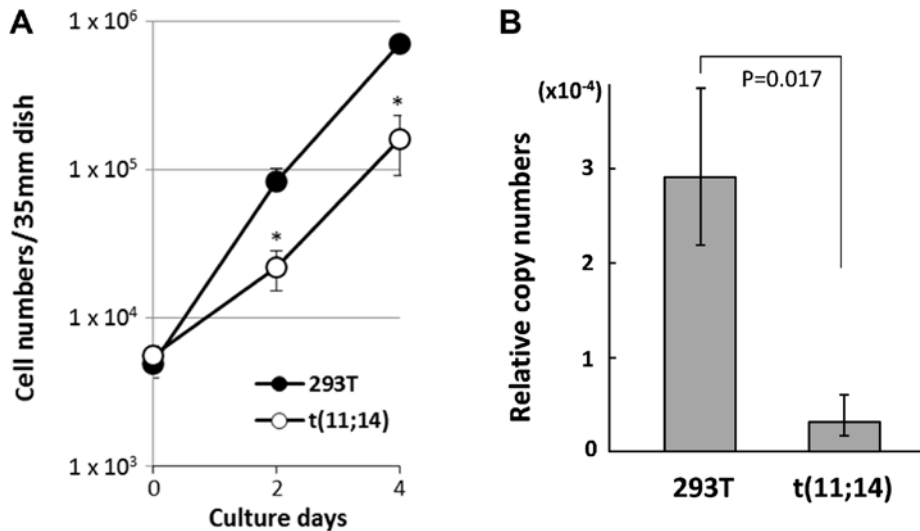


Figure 5. Characteristics of 293T cells harboring t(11;14). (A) Growth curves of t(11;14) 293T cells and parental cells. Viable cell numbers are indicated on days 0, 2, and 4 (n=3). Error bars indicate the standard deviation. *P<0.05 vs. 293T. (B) Reverse transcription-quantitative PCR analysis of *CCND1*. Relative copy numbers were calculated using *GAPDH* as a reference (n=3). CCND1, cyclin D1.

CRISPR/Cas9 (22-27), we encountered growth repression in the non-B lymphocyte target cells, which could have been associated with the transcriptionally silent *IgH* gene. These data suggest that selection pressure specific to translocation-positive cells is important to isolate the cells with such growth-suppressing translocations.

Recent reports have described efficient induction of targeted chromosomal translocation by introduction of a HDR template DNA which mimics translocation junction sequences (27,36). The template DNA carries a 5'-translocation donor gene fragment and 3'-recipient gene fragment

separated by a selection marker, and is introduced into cells with routine translocation site-specific CRISPR/Cas9 vectors. After the two target sequences are specifically cut by Cas9s, breakpoints are repaired by HDR using the template DNA to form chromosomal translocation. Furthermore, the use of HSVtk for negative selection of off-target recombination of template DNA (37), knockout of p53 to suppress apoptotic cell death (38,39), and addition of NHEJ inhibitors to shift DNA double strand break repair system to HDR (40-42) also enhance HDR-template mediated genome editing. As application of these techniques can accelerate selective induction

of difficult chromosomal translocations, we are planning to explore use of these techniques in combinations for future studies.

Although *CCND1* expression in cells with translocations is thought to be associated with the transcriptional silence of *IgH* in cells other than B lymphocytes, we were able to obtain cells with t(11;14), suggesting that we should be able to induce this type of translocation in other cells. In addition, different types of immunoglobulin-associated translocations observed in B lymphocytic malignancies could be induced using a similar CRISPR/Cas9 system. For studying the process of myelomagenesis in the viewpoint of *IgH* enhancer-driven *CCND1* overexpression, we plan to induce t(11;14) in B lymphocyte-derived iPSC cells (BiPSCs) in which *IgH* genes are silent (43) using this technique. As we have already confirmed that our BiPSCs can be differentiated into hematopoietic stem cells (HSCs), we will check if t(11;14)-carrying BiPSCs are also capable of differentiating into HSCs and B lymphocyte lineage *in vitro*. Moreover, we will analyze the possible function of t(11;14) and *CCND1* overexpression on B-cell differentiation and tumor development after transplantation into mouse bone marrow by comparing t(11;14)-BiPSC and parental BiPSC.

Acknowledgements

Not applicable.

Funding

The present study was supported in part by grants-in-aid for Scientific Research (grant nos. 15K00543 and 16K18424) from the Japanese Ministry of Education, Culture, Sports, Science, and Technology.

Availability of data and materials

All data generated or analyzed during this study are included in this published article.

Authors' contributions

NT designed and performed the study. YA conducted the growth analysis and RT-qPCR. AY, YY and MS contributed to the cell culture and gene delivery experiments. AK and FK were involved in the design and construction of the CRISPR vectors. KK was involved in the experimental design. AS conceived and designed the study. All authors read and approved the manuscript, and agreed to be accountable for all aspects of the work in ensuring that questions related to the accuracy or integrity of any part of the work are appropriately investigated and resolved.

Ethics approval and consent to participate

Not applicable.

Patient consent for publication

Not applicable.

Competing interests

The authors declare that they have no competing interests.

References

- Rabbitts TH: Chromosomal translocations in human cancer. *Nature* 372: 143-149, 1994.
- Nambiar M, Kari V and Raghavan SC: Chromosomal translocations in cancer. *Biochim Biophys Acta* 1786: 139-152, 2008.
- Lieber MR: Mechanisms of human lymphoid chromosomal translocations. *Nat Rev Cancer* 16: 387-398, 2016.
- Chesi M, Bergsagel PL, Brents LA, Smith CM, Gerhard DS and Kuehl WM: Dysregulation of cyclin D1 by translocation into an IgH gamma switch region in two multiple myeloma cell lines. *Blood* 88: 674-681, 1996.
- Chesi M, Nardini E, Brents LA, Schrock E, Ried T, Kuehl WM and Bergsagel PL: Frequent translocation t(4;14)(p16.3;q32.3) in multiple myeloma is associated with increased expression and activating mutations of fibroblast growth factor receptor 3. *Nat Genet* 16: 260-264, 1997.
- Chesi M, Bergsagel PL, Shonukan OO, Martelli ML, Brents LA, Chen T, Schrock E, Ried T and Kuehl WM: Frequent dysregulation of the c-maf proto-oncogene at 16q23 by translocation to an Ig locus in multiple myeloma. *Blood* 91: 4457-4463, 1998.
- Inaba T, Matsushime H, Valentine M, Roussel MF, Sherr CJ and Look AT: Genomic organization, chromosomal localization, and independent expression of human cyclin D genes. *Genomics* 13: 565-574, 1992.
- Szepietowski P, Perucca-Lostanlen D and Gaudray P: Mapping genes according to their amplification status in tumor cells: Contribution to the map of 11q13. *Genomics* 16: 745-750, 1993.
- Sherr CJ: Mammalian G1 cyclins. *Cell* 73: 1059-1065, 1993.
- Fonseca R, Blood EA, Oken MM, Kyle RA, Dewald GW, Bailey RJ, Van Wier SA, Henderson KJ, Hoyer JD, Harrington D, *et al*: Myeloma and the t(11;14)(q13;q32); evidence for a biologically defined unique subset of patients. *Blood* 99: 3735-3741, 2002.
- Fenton JA, Pratt G, Rothwell DG, Rawstron AC and Morgan GJ: Translocation t(11;14) in multiple myeloma: Analysis of translocation breakpoints on der(11) and der(14) chromosomes suggests complex molecular mechanisms of recombination. *Genes Chromosomes Cancer* 39: 151-155, 2004.
- Walker BA, Wardell CP, Johnson DC, Kaiser MF, Begum DB, Dahir NB, Ross FM, Davies FE, Gonzalez D and Morgan GJ: Characterization of IGH locus breakpoints in multiple myeloma indicates a subset of translocations appear to occur in pregerminal center B cells. *Blood* 121: 3413-3419, 2013.
- Xu Z, Zan H, Pone EJ, Mai T and Casali P: Immunoglobulin class-switch DNA recombination: Induction, targeting and beyond. *Nat Rev Immunol* 12: 517-531, 2012.
- Casellas R, Basu U, Yewdell WT, Chaudhuri J, Robbiani DF and Di Noia JM: Mutations, kataegis and translocations in B cells: Understanding AID promiscuous activity. *Nat Rev Immunol* 16: 164-176, 2016.
- Nambiar M and Raghavan SC: How does DNA break during chromosomal translocations? *Nucleic Acids Res* 39: 5813-5825, 2011.
- Van der Oost J: Molecular biology. New tool for genome surgery. *Science* 339: 768-770, 2013.
- Gaj T, Gersbach CA and Barbas CF III: ZFN, TALEN, and CRISPR/Cas-based methods for genome engineering. *Trends Biotechnol* 31: 397-405, 2013.
- Jinek M, Chylinski K, Fonfara I, Hauer M, Doudna JA and Charpentier E: A programmable dual-RNA-guided DNA endonuclease in adaptive bacterial immunity. *Science* 337: 816-821, 2012.
- Cong L, Ran FA, Cox D, Lin S, Barretto R, Habib N, Hsu PD, Wu X, Jiang W, Marraffini LA and Zhang F: Multiplex genome engineering using CRISPR/Cas systems. *Science* 339: 819-823, 2013.
- Mali P, Yang L, Esvelt KM, Aach J, Guell M, DiCarlo JE, Norville JE and Church GM: RNA-guided human genome engineering via Cas9. *Science* 339: 823-826, 2013.
- Moreno-Mateos MA, Vejnar CE, Beaudoin JD, Fernandez JP, Mis EK, Khokha MK and Giraldez AJ: CRISPRscan: Designing highly efficient sgRNAs for CRISPR-Cas9 targeting *in vivo*. *Nat Methods* 12: 982-988, 2015.
- Choi PS and Meyerson M: Targeted genomic rearrangements using CRISPR/Cas technology. *Nat Commun* 5: 3728, 2014.

23. Breese EH, Buechele C, Dawson C, Cleary ML and Porteus MH: Use of genome engineering to create patient specific MLL translocations in primary human hematopoietic stem and progenitor cells. *PLoS One* 10: e0136644, 2015.
24. Jiang J, Zhang L, Zhou X, Chen X, Huang G, Li F, Wang R, Wu N, Yan Y, Tong C, *et al*: Induction of site-specific chromosomal translocations in embryonic stem cells by CRISPR/Cas9. *Sci Rep* 6: 21918, 2016.
25. Lekontsev S, Aligianni S, Lapao A and Bürckstummer T: Efficient generation and reversion of chromosomal translocations using CRISPR/Cas technology. *BMC Genomics* 17: 739, 2016.
26. Reimer J, Knoss S, Labuhn M, Charpentier EM, Gohring G, Schlegelberger B, Klusmann JH and Heckl D: CRISPR-Cas9-induced t(11;19)/MLL-ENL translocations initiate leukemia in human hematopoietic progenitor cells in vivo. *Haematologica* 102: 1558-1566, 2017.
27. Vanoli F, Tomishima M, Feng W, Lamribet K, Babin L, Brunet E and Jasin M: CRISPR-Cas9-guided oncogenic chromosomal translocations with conditional fusion protein expression in human mesenchymal cells. *Proc Natl Acad Sci USA* 114: 3696-3701, 2017.
28. Mashiko D, Fujihara Y, Satouh Y, Miyata H, Isotani A and Ikawa M: Generation of mutant mice by pronuclear injection of circular plasmid expressing Cas9 and single guided RNA. *Sci Rep* 3: 3355, 2013.
29. Cepko C: Large-scale preparation and concentration of retrovirus stocks. *Curr Protoc Mol Biol*. Chapter 9: Unit 0.12, 1997. doi: 10.1002/0471142727.mb0912s37.
30. Doench JG, Fusi N, Sullender M, Hegde M, Vaimberg EW, Donovan KF, Smith I, Tothova Z, Wilen C, Orchard R, *et al*: Optimized sgRNA design to maximize activity and minimize off-target effects of CRISPR-Cas9. *Nat Biotechnol* 34: 184-191, 2016.
31. Livak KJ and Schmittgen TD: Analysis of relative gene expression data using real-time quantitative PCR and the 2(-Delta Delta C(T)) method. *Methods* 25: 402-408, 2001.
32. Ronchetti D, Finelli P, Richelda R, Baldini L, Rocchi M, Viggiano L, Cuneo A, Bogni S, Fabris S, Lombardi L, *et al*: Molecular analysis of 11q13 breakpoints in multiple myeloma. *Blood* 93: 1330-1337, 1999.
33. Jhunjhunwala S, van Zelm MC, Peak MM, Cutchin S, Riblet R, van Dongen JJ, Grosveld FG, Knoch TA and Murre C: The 3D structure of the immunoglobulin heavy-chain locus: Implications for long-range genomic interactions. *Cell* 133: 265-279, 2008.
34. Zwijsen RM, Klompmaker R, Wientjens EB, Kristel PM, van der Burg B and Michalides RJ: cyclin D1 triggers autonomous growth of breast cancer cells by governing cell cycle exit. *Mol Cell Biol* 16: 2554-2560, 1996.
35. Janssen JW, Vaandrager JW, Heuser T, Jauch A, Kluin PM, Geelen E, Bergsagel PL, Kuehl WM, Drexler HG, Otsuki T, *et al*: Concurrent activation of a novel putative transforming gene, *myeov*, and cyclin D1 in a subset of multiple myeloma cell lines with t(11;14)(q13;q32). *Blood* 95: 2691-2698, 2000.
36. Spraggon L, Martelotto LG, Hmeljak J, Hitchman TD, Wang J, Wang L, Slotkin EK, Fan PD, Reis-Filho JS and Ladanyi M: Generation of conditional oncogenic chromosomal translocations using CRISPR-Cas9 genomic editing and homology-directed repair. *J Pathol* 242: 102-112, 2017.
37. Gondo Y, Nakamura K, Nakao K, Sasaoka T, Ito K, Kimura M and Katsuki M: Gene replacement of the p53 gene with the lacZ gene in mouse embryonic stem cells and mice by using two steps of homologous recombination. *Biochem Biophys Res Commun* 202: 830-837, 1994.
38. Haapaniemi E, Botla S, Persson J, Schmierer B and Taipale J: CRISPR-Cas9 genome editing induces a p53-mediated DNA damage response. *Nat Med* 24: 927-930, 2018.
39. Ihry RJ, Worringer KA, Salick MR, Frias E, Ho D, Theriault K, Kommineni S, Chen J, Sondey M, Ye C, *et al*: p53 inhibits CRISPR-Cas9 engineering in human pluripotent stem cells. *Nat Med* 24: 939-946, 2018.
40. Yu C, Liu Y, Ma T, Liu K, Xu S, Zhang Y, Liu H, La Russa M, Xie M, Ding S and Qi LS: Small molecules enhance CRISPR genome editing in pluripotent stem cells. *Cell Stem Cell* 16: 142-147, 2015.
41. Song J, Yang D, Xu J, Zhu T, Chen YE and Zhang J: RS-1 enhances CRISPR/Cas9- and TALEN-mediated knock-in efficiency. *Nat Commun* 7: 10548, 2016.
42. Li G, Zhang X, Zhong C, Mo J, Quan R, Yang J, Liu D, Li Z, Yang H and Wu Z: Small molecules enhance CRISPR/Cas9-mediated homology-directed genome editing in primary cells. *Sci Rep* 7: 8943, 2017.
43. Kawamura F, Inaki M, Katafuchi A, Abe Y, Tsuyama N, Kurosu Y, Yanagi A, Higuchi M, Muto S, Yamaura T, *et al*: Establishment of induced pluripotent stem cells from normal B cells and inducing AID expression in their differentiation into hematopoietic progenitor cells. *Sci Rep* 7: 1659, 2017.



This work is licensed under a Creative Commons Attribution-NonCommercial-NoDerivatives 4.0 International (CC BY-NC-ND 4.0) License.